Real space renormalization group approach to the random field Ising model

1993 J. Phys. A: Math. Gen. 26 3093

(http://iopscience.iop.org/0305-4470/26/13/014)

J. Phys. A: Math. Gen. 26 (1993) 3093–3103. Printed in the UK

Real space renormalization group approach to the random field Ising model

I Dayan†, M Schwartz‡ and A P Young§

† Physics Department, Bar-Ilan University, Ramat Gan, Israel

‡ School of Physics and Astronomy, Tel Aviv University, Ramat Aviv, Tel Aviv, 69978 Israel

§ Physics Department, University of California Santa Cruz, Santa Cruz, CA 95064, USA

Received 13 January 1993

Abstract. We discuss results from two types of real space renormalization group (RSRG) calculations applied to the random field Ising model in three dimensions. Starting from a lattice of size L, the RSRG is used to reduce the lattice to a size $L = 2$, on which the trace is done exactly. In this way, thermodynamic properties, such as the magnetization and susceptibility, can be determined approximately. We find that, for a given size, the susceptibility increases as the temperature, T, is reduced down to the transition temperature, T_c, and becomes essentially independent of temperature below T_c. Both in the vicinity of T_c and at lower temperatures, there are large sample-to-sample fluctuations in the susceptibility which grow with increasing system size. We interpret these results in terms of the droplet theory of the transition.

1. Introduction

The random field Ising model (RFIM) has been extensively studied, both theoretically and experimentally [1, 2]. While there is general agreement that a phase transition to an ordered state occurs in three dimensions [3], the nature of the transition is poorly understood. For example, it is not definitely established whether the transition is second order or first order with large fluctuations. Assuming that the transition is second order, the values of the critical exponents are not known with any precision, and estimates from experiment and numerical work appear to be inconsistent.

Difficulties in the theory stem from the RFIM being a frustrated system which has a complicated (free) energy landscape with more than one inequivalent minimum. A scaling (droplet) theory based on this picture has been developed by Villain [4] and Fisher [5] (see also Bray and Moore [6]). According to these ideas, a system of size L at $T = T_c$ is most likely to have just one minimum which is thermally populated, but there is a small probability, of order $L^{-\theta}$, that there is a second minimum whose (total) free energy is within of order $k_B T$ of the lowest minimum. Here $\theta(> 0)$ is a critical exponent. When there are two degenerate minima the susceptibility is greatly enhanced, as we will see in section 2. We also expect a similar picture to hold below T_c, but now θ, rather than being a non-trivial critical exponent, should be equal to $d/2$ as also shown in section 2.

In this paper we calculate the susceptibility and other quantities of the RFIM using real space renormalization group (RSRG) methods. We find that the susceptibility has large sample-to-sample fluctuations of the form predicted by the droplet theory both at and below T_c. However, the values of θ at and below T_c are indistinguishable within the accuracy of the calculation, which indicates that the transition is close to first order.

0305-4470/93/133093+11$07.50

2. The model and some of its properties

The Hamiltonian is given by

$$\mathcal{H} = -\sum_{\langle i,j \rangle} J_{i,j} S_i S_j - \sum_{i=1}^{N} h_i S_i \tag{1}$$

where the interactions, $J_{i,j}$, are between nearest neighbours on a simple cubic lattice with $N = L^3$ sites, the Ising spins, S_i, take values ± 1, and the fields, h_i, are chosen to have zero mean and standard deviation equal to h_r. We are interested in the susceptibility χ, which is related to spin correlation functions by the standard expression

$$\chi = \frac{1}{NT} \sum_{i,j=1}^{N} (\langle S_i S_j \rangle - \langle S_i \rangle \langle S_j \rangle) \tag{2}$$

where $\langle \cdots \rangle$ denotes a thermal average. Another quantity of interest will be the 'disconnected' susceptibility, defined by

$$\chi_{\text{dis}} = \frac{1}{N} \sum_{i,j=1}^{N} \langle S_i \rangle \langle S_j \rangle. \tag{3}$$

We now discuss the sample-to-sample fluctuations in the susceptibility at T_c. According to the droplet theory [4, 5] most samples have only one thermally populated minimum. For these samples, the two terms in equation (2) almost cancel. More precisely, while each term separately has the divergence of χ_{dis}, i.e.

$$\chi_{\text{dis}} \sim L^{4-\bar{\eta}} \qquad (T = T_c) \tag{4}$$

the difference is given by

$$\chi \sim L^{2-\eta} \qquad (T = T_c) \qquad (\text{prob.} \sim 1). \tag{5}$$

Here, η and $\bar{\eta}$ are critical exponents and, according to the droplet theory, θ is related to them by

$$\theta = 2 - \bar{\eta} + \eta. \tag{6}$$

The Schwartz–Soffer inequality [7], when applied to a finite system, predicts $[\chi(L)]_{\text{av}} \leqslant h_r^{-1} \{[\chi_{\text{dis}}(L)]_{\text{av}}\}^{1/2}$, where $[\cdots]_{\text{av}}$ denotes an average over random field configurations. Therefore, the cancellation of the most divergent terms in the susceptibility is rigorously true on average.

The droplet theory also predicts that there is a probability $\sim L^{-\theta}$ that a sample has more than one minimum which is thermally populated and, for these samples, the two terms in equation (2) do *not* cancel, but the difference is of the same order as each term, i.e.

$$\chi \sim L^{4-\bar{\eta}} \qquad (T = T_c) \qquad (\text{prob.} \sim L^{-\theta}). \tag{7}$$

Hence there is a very small probability that the susceptibility is much larger than the typical value. On increasing the lattice size, the probability of obtaining one of these rare samples

decreases but the susceptibility of a rare sample, relative to a typical value, gets larger. Averaging over samples, and using equations (5) and (7), one sees that for the first moment, $[\chi]_{av}$, both the typical and rare samples give a comparable contribution,

$$[\chi]_{av} \sim L^{2-\eta} \qquad (T = T_c) \tag{8}$$

but higher moments are dominated by the rare samples, so, for example,

$$[\chi^2]_{av} \sim L^{6-\bar{\eta}-\eta} \qquad (T = T_c) \tag{9}$$

which is much larger than $[\chi]^2_{av}$. At T_c, then, χ is highly non-self-averaging. Nonetheless, we expect that χ *will* be self-averaging sufficiently far above T_c that $\xi \ll L$, where ξ is the correlation length, because, in this case, the system can be divided into essentially independent regions of size ξ and any measurement on the whole sample will be an average over these regions.

Alternatively, one can discuss the distribution of χ rather than its moments. This is expected to be very broad, with a most probable value of order $L^{2-\eta}$ and a tail extending out to values of order $L^{4-\bar{\eta}}$. We shall see that these features of the distribution and its moments are reproduced by the RSRG calculations described in the next two sections. Note that all samples give a value for χ_{dis} of order $L^{4-\bar{\eta}}$, as in equation (4), so this is also true for the average value, i.e.

$$[\chi_{dis}]_{av} \sim L^{4-\bar{\eta}} \qquad (T = T_c). \tag{10}$$

In the ordered phase, we expect that the behaviour of χ and χ_{dis} will be of the form given in equations (4), (5) and (7), for $T \neq T_c$, but with values for the exponents which can be determined from elementary considerations as follows. Below T_c there is long-range order so $\chi_{dis} \sim L^d$, i.e. $\bar{\eta} = 4 - d$ (= 1 for $d = 3$). It is reasonable to expect that, at low temperatures, the differences in the free energies of the minima should be of order $L^{d/2}$ (where d is the dimension: $d = 3$ here), since this is the difference in free energy between the state with all spins up and the state with all spins down. (To see this note that the sum of the random fields in a sample is of order the square root of the number of sites.) Assuming a constant density of states for the free energy difference (as in the theory of Fisher [5] for the situation at T_c) this gives a probability of order $L^{-d/2}$ that the two lowest minima differ in free energy by less than k_BT and so $\theta = d/2$. Finally, following Fisher [5] we assume that the whole curve of the free energy against magnetization scales with size as L^θ, so the susceptibility, which is related to the curvature at the minima, varies as $\chi \sim L^{d/2}$, and hence $\eta = (4 - d)/2$. The exponents for $T < T_c$, i.e.

$$\eta = 0.5 \qquad \bar{\eta} = 1.0 \qquad \theta = 1.5 \tag{11}$$

(in $d = 3$) should also be valid *at* T_c if the transition is first order, because, in this case, the system is already ordered at T_c. Note that when equation (11) is valid, the Schwartz–Soffer [7] inequality,

$$\eta \geqslant \tfrac{1}{2}\bar{\eta} \tag{12}$$

is satisfied as an equality.

3. Casher–Schwartz approximation

In this section and the next section, we apply two approximate RSRG transformations, the Casher–Schwartz (CS) approximation [8] and the Migdal–Kadanoff (MK) approximation [9, 10] to the RFIS. Both procedures generate correlations among the renormalized coupling constants. Usually, such correlations are neglected, although, as demonstrated for the random bond system, it may be appropriate to take the correlations into account as contributions to an effective renormalized variance [11]. Here we do not neglect these correlations but rather start from a *finite* lattice of linear size L, which must be a power of 2, i.e. $L = 2^n$, with a given realization of the random fields. We use the two RSRG methods to reduce the size of the lattice to $L = 2$, for which the trace can be done exactly. This approach has the advantage that all correlations are kept, but has the disadvantage that only a finite number of iterations, $n-1$, can be performed. In the more conventional approach, in which one makes additional approximations such as neglect of correlations, one can iterate an arbitrary number of times.

The CS method considered in this section is only slightly more complicated to implement than the MK method to be considered in the next section. Its advantages are that the generated couplings remain symmetric in all space dimensions and that the critical exponents obtained for the pure system are in better agreement with the exact values for the pure systems. A detailed description of the method can be found in [8] so here we just give a short account of it. We start from a cubic lattice with periodic boundary conditions and divide it into two sublattices, such that all the neighbours of a site are on the other sublattice. Summing over the spins one of the sub-lattices the result is a spin Hamiltonian on a BCC lattice, which contains single-site (random field) terms, two spin couplings and higher odd and even multi-spin interactions. The multi-spin interactions are neglected, and some of the two-spin interactions are replaced by other two-spin interactions in such a way that the small momentum form of the original pure Hamiltonian and the new pure effective one, are identical. Summation over the body centre spins can be done exactly. The result is a simple cubic system that is brought, by applying the above method again, to its original form, i.e. a nearest-neighbour interaction and a random field.

We consider the case that corresponds to the experimental situation, where the interactions and random fields are kept fixed and only the temperature is varied. We therefore set $J_{i,j} = 1$ in equation (1) and choose a realization of the random field with $h_r = 1$.

We calculate the configurational average of the susceptibility by going through the following steps:

(i) A fixed uniform field is added to a *given* realization of the random field.

(ii) We apply the number of renormalization steps needed to reduce the size of the system to $L = 2$.

(iii) The *space* average magnetization of the remaining spins is calculated exactly.

(iv) The configuration average is then performed by repeating the previous steps for many random field configurations. For a finite system the average must be zero for $h = 0$ because of the basic reflection symmetry of the system. To preserve this symmetry, when only a finite number of configurations is used in the average, we also include the mirror image of each random field realization.

(v) The average susceptibility $[\chi]_{\mathrm{av}}$ is

$$[\chi]_{\mathrm{av}} = \frac{\partial}{\partial h}[M(h)]_{\mathrm{av}}\bigg|_{h=0} \tag{13}$$

but, since $[M(0)]_{av} = 0$, we actually calculate

$$[\chi]_{av} = \lim_{h \to 0} \frac{[M(h)]_{av}}{h}. \tag{14}$$

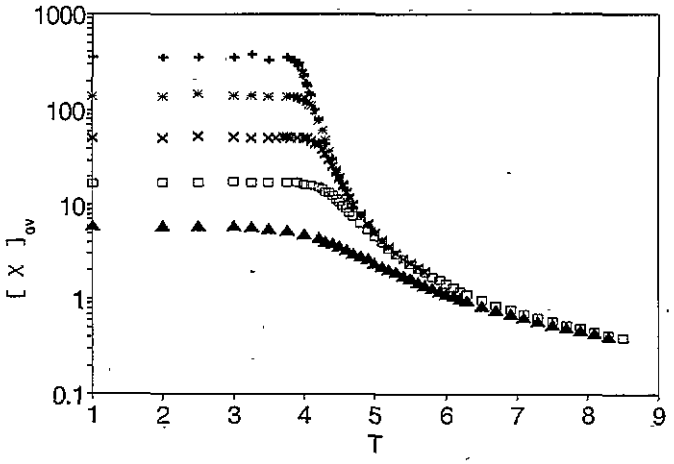

Figure 1. A plot of the average susceptibility against temperature for sizes between $L = 4$ and $L = 64$ using the CS approximation with $h_r = 1$ and the nearest-neighbour interaction given by $J_{i,j} = 1$.

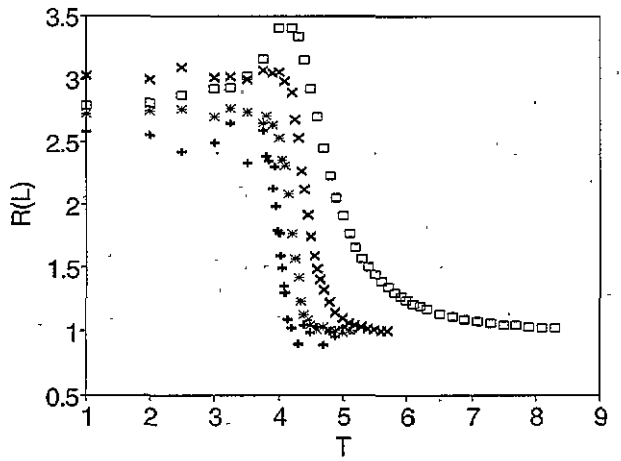

Figure 2. A plot of $R(L) \equiv [\chi(2L, T)]_{av}/[\chi(L, T)]_{av}$ for various sizes and temperatures using the CS approximation.

A word of caution is in place here concerning the numerical derivative at $h = 0$. We must choose h small enough so that $[M(h)]_{av}$ is linear in h. The difficulty is that, below the transition, the size of the region shrinks to zero when the size of the system tends to infinity, but for h too small we encounter numerical problems from round off errors. Fortunately,

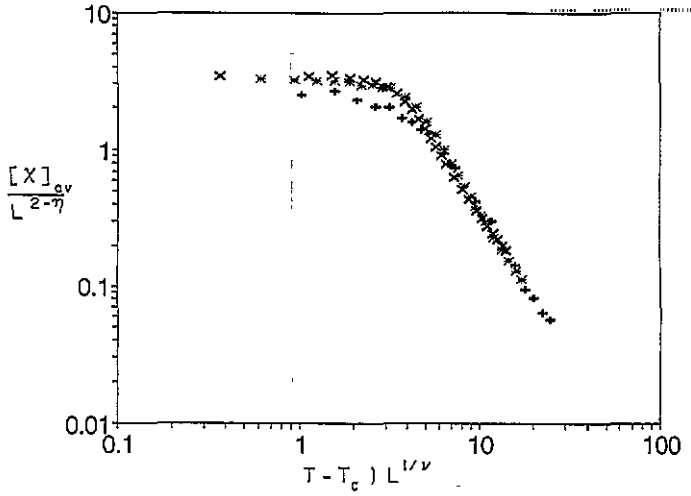

Figure 3. Scaling plot for the average susceptilibity, as discussed in the text, for the CS approximation. The exponent values are $\eta = 0.53$ and $\nu = 1.36$, and the transition temperature is taken to be $T_c = 3.85$.

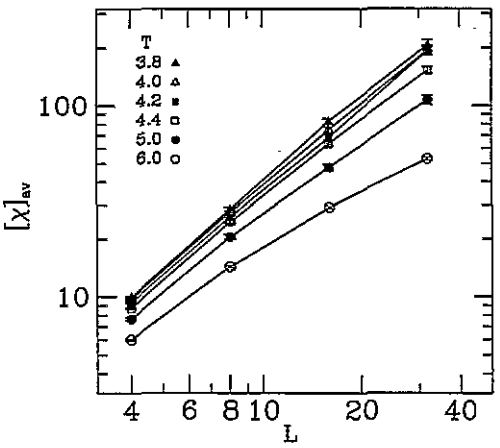

Figure 4. The average susceptibility as a function of L on a log–log plot for different temperatures for the MK approximation with $h_r/T = 0.5$ and the nearest-neighbour interactions in the different directions given by $J_x = 2J_y = 4J_z$ with $J_y = 1$.

we were able to meet both requirements, except possibly for the the data below T_c for the largest size considered, $L = 64$ (see the comments below on figure 3).

The susceptibility is presented in figure 1 for different sizes as a function of temperature. In the low-temperature regime we see that, excluding $L = 4$, the ratio $R(L) \equiv [\chi(2L, T)]_{av}/[\chi(L, T)]_{av}$ is almost temperature independent, as shown in figure 2. Furthermore, for large L, R also becomes almost L independent, which implies that $[\chi]_{av}$ varies with a power of L. Fitting to equation (8) we find $\eta \approx 0.53$ with about 10% accuracy, which is close to the value $\eta = 0.5$ expected at a first-order transition, see equation (11). To obtain the other critical exponents we use the finite-size scaling form

$$[\chi(L, T)]_{av} = L^{2-\eta}\tilde{\chi}(L^{1/\nu}(T - T_c)) \tag{15}$$

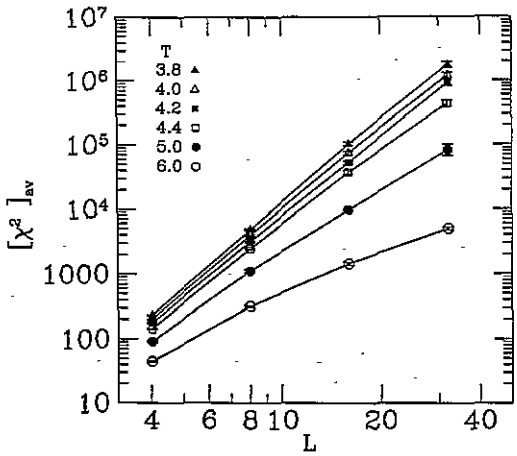

Figure 5. The mean square susceptibility as a function of L on a log–log plot for different temperatures for the MK approximation.

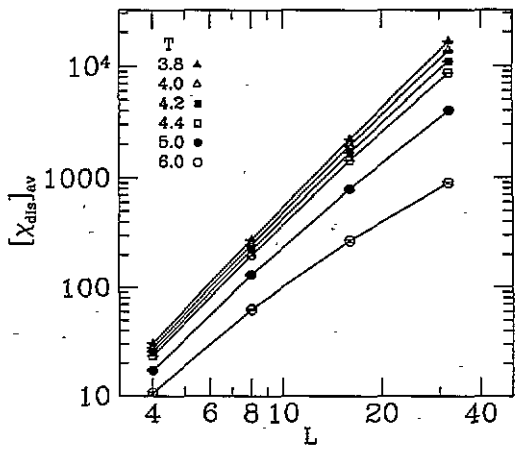

Figure 6. The disconnected susceptibility as a function of L on a log–log plot for different temperatures for the MK approximation.

where ν is the exponent which describes the divergence of the correlation length with temperature. The susceptibility exponent, γ is then given by $\gamma = (2-\eta)\nu$. We guess a value for γ, set $\eta = 0.53$, and determine ν from $\nu = \gamma/(2-\eta)$. Next we estimate the best T_c for this γ by requiring that the data for the susceptibility of the largest systems a little above T_c (where finite-size effects should be unimportant) are of the form $(T-T_c)^{-\gamma}$. With these parameter values, we plot $[\chi(L,T)]_{av}/L^{2-\eta}$ as a function of $L^{1/\nu}(T-T_c)$. This procedure is repeated for several values of γ until we get the best data collapse. Using the sizes $L = 16$, 32 and 64 we found that the best fit is obtained for $\gamma = 1.9$–2.2. Within that range it is impossible to prefer one value over another. The fit for $\gamma = 2$ is shown in figure 3. The results for the $L = 64$ system are a little low at low temperatures, probably because the value of h used for the numerical differentiation was too big (see the comments above on difficulties in choosing the right value of h). However, the critical exponents are determined from the data above T_c, where the different graphs coincide.

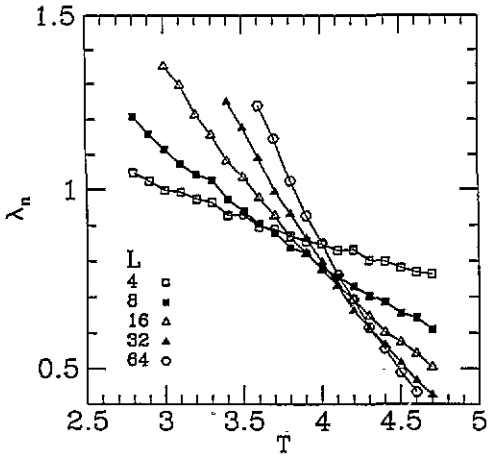

Figure 7. The ratio, λ_n, as defined in the text, for various sizes, $L \equiv 2^{n+1}$, for the MK approximation. The curves are expected to intersect at T_c.

We can also estimate the specific heat exponent, α, from the scaling law $\alpha+2\beta+\gamma=2$ where β is the order parameter exponent. In the next section we find that $\beta \simeq 0$, consistent with results of Ogielski [12], so, using the above value of γ, one finds that α is very small, or even negative. As a self-consistency check, we have also calculated the average energy associated with the random field (in the absence of an external uniform field). This is done by the same decimation procedure as before. The difference is that instead of calculating the space average of $\langle S_i \rangle$ over the spins in the $L=2$ lattice, we calculate $\mathcal{E}_F = \sum h_i \langle S_i \rangle$ summed over those spins. Note that h_i is the original field, since the renormalization scheme is just a way of calculating the thermal average of the spin $\langle S_i \rangle$. We expect that the part of the energy associated with the random field scales in the same way as the total energy. The temperature derivative of $\mathcal{E}_F$ is very noisy but shows no tendency to diverge at T_c. This is consistent with the above estimate for α obtained from scaling laws, and, given the noise in the data, it may also be consistent with the experimental result [13] showing a weak logarithmic divergence, $\alpha = 0$.

4. Migdal–Kadanoff approximation

We now discuss our second approximation, due to Migdal and Kadanoff (MK). This is a very simple method, which has, nonetheless, been quite successful when applied to frustrated systems. For example, the MK method was the first to give the (apparently correct) result that there is a transition in the three-dimensional Ising spin glass but not in the two-dimensional spin glass [14, 15]. The repeated MK transformation enables us to keep track of the spin-independent term in the Hamiltonian at each stage, so we can compute the free energy and hence its derivatives such as the magnetization and the susceptibility. Since the spin-independent term is evaluated analytically we can evaluate χ directly at $h=0$, where h is a uniform field, without needing to take a finite difference of the magnetization at two field values, as was necessary for the CS approximation in the previous section.

The MK method has been extensively discussed elsewhere [9, 10] so we will not go into details here. Basically one moves bonds around so that the trace can be done over spins which are connected to only two neighbours. We use a scale factor of $b=2$ so that the

size of the lattice is reduced by a factor of 2 each time. The method does not mix the bonds in the different directions and, in fact, treats the bonds in the x, y and z directions inequivalently. As a result, the pure system (i.e. without random fields) has different fixed-point equations for the x, y and z bonds. In order that one obtains a fixed point at the same temperature for the bonds in each direction, one must choose the bonds in different directions to have different values in the original Hamiltonian, namely $J_x = 2J_y = 4J_z$.

For the pure system, this ratio is maintained by the transformation. We also adopt this choice of bonds in the initial Hamiltonian for the random field case, and work in units where $J_y = 1$. In this section the ratio h_r/T is kept constant, which corresponds to working on a line at a fixed angle through the origin in the h–T plane. We use the value $h_r/T = 0.5$. Note that in the previous section, it was h_r/J (with $J = 1$) that was kept constant.

In applying the bond-moving MK scheme to systems with fields one also needs to decide how much of the field on a site is moved, if a bond attached to that site is moved. In order to recover the correct low-temperature behaviour, it is necessary to associate an equal fraction of the field with each of the bonds from the site, and move that part of the field along with the bond [16].

In figures 4–6 results for $[\chi]_{av}$, $[\chi^2]_{av}$ and $[\chi_{dis}]_{av}$ are shown plotted against L on a double logarithmic scale for different temperatures. At high temperatures, there is curvature in the data indicating that the results will saturate for larger sizes. For temperatures at and below about 4.2, we see power-law behaviour, with an exponent which does not change significantly at lower temperatures. It is therefore difficult to distinguish the low-temperature region from the critical region.

We attempted to determine the location of the critical point by looking at how $K_n \equiv ([h_i^2]_{av})^{1/2}/J$ varies with n, the number of iterations. Here $J = (0.5[J_x] + [J_y] + 2[J_z])/3$, where $[J_x]$ is the average value of the nearest-neighbour interaction in the x direction, averaged over both sites and field configurations. We calculated this ratio, both for the original Hamiltonian on a lattice of size L and in the lattice rescaled down to a linear size of 2. Dividing the latter quantity by the former, we get $\lambda_n \equiv K_n/K_0$ for a number of iterations equal to $n = \log_2(L) - 1$. In the disordered phase, the effective coupling λ_n goes to zero with increasing n, while at the critical point, the coupling goes to a fixed point value, so λ_n becomes independent of n. In the ordered phase, λ_n is expected to diverge. Hence the critical point can be located by looking for the intersection of curves of λ against T for different sizes. We plot this ratio in figure 7. Unfortunately, the curves do not intersect at a single point: rather the intersection of neighbouring values of n occurs at somewhat higher temperatures as n increases. Presumably one would need to do larger sizes to determine T_c precisely. However, from figure 7 it appears that T_c cannot be much less than about 4.2 and, from the data for in figures 4–6, T_c cannot be much greater than this since the data start to show curvature. Hence we estimate $T_c \simeq 4.2$. Our conclusions are not very sensitive to the precise value of T_c.

From the slopes of the curves for $[\chi]_{av}$ and $[\chi_{dis}]_{av}$ at $T = 4.2$ we find $\eta = 0.56$ and $\bar{\eta} = 1.0$. As a consistency check on the droplet picture we use equation (9) to determine the expected exponent for $[\chi^2]_{av}$ obtaining 4.44. The actual value, obtained from figure 5, is 4.43, which is in excellent agreement. This shows that the RSRG approximation confirms the droplet picture. Note that $\bar{\eta} = 1.0$ gives $\beta = 0$, using the scaling law $\beta = (d - 4 + \bar{\eta})\nu/2$. The best estimate for β so far is probably that of Ogielski [12], who found $\beta \approx 0.1$, which is also close to zero.

Histograms of the values of χ at $T = 4.2$ for $L = 32$ and 16 are shown in figures 8 and 9. The results show the expected behaviour of a peak at rather small values of χ and a long tail (notice the horizontal scale is logarithmic), extending to much larger values. The

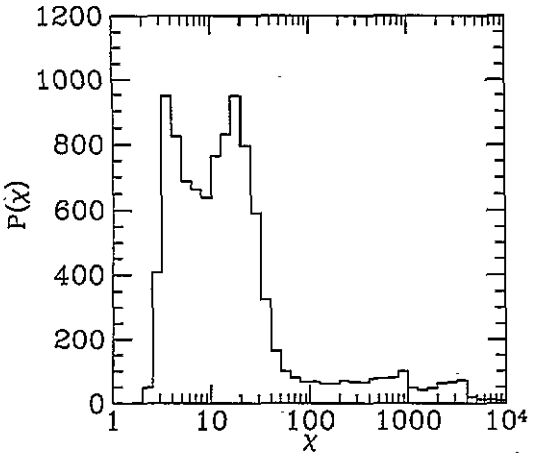

Figure 8. Histogram of the susceptibilities of 10 000 samples for $L = 32$, $T = 4.2$ for the MK approximation. Note the long tail in the distribution.

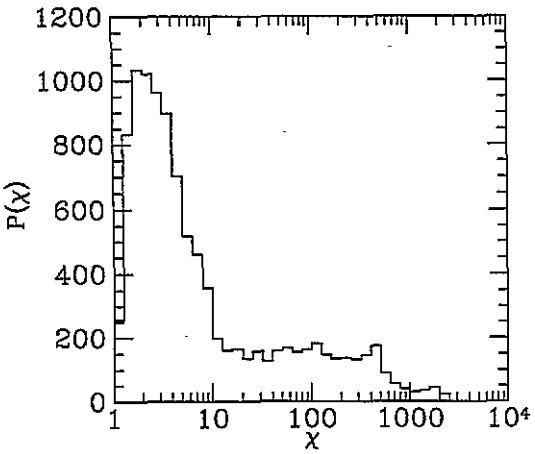

Figure 9. Histogram of the susceptibilities of 10 000 samples for $L = 16$, $T = 4.2$ for the MK approximation. Note the long tail in the distribution.

the tail is seen to be longer for the larger size, as expected.

From our results we are unable to detect, within the accuracy of the data and the limitations of the finite sizes, any difference between the exponents at and below T_c. This indicates that the transition is close to first order as discussed in section 2.

5. Conclusions

We have applied two RSRG approximations to study the susceptibility of the random field Ising model. We find that there are large sample-to-sample fluctuations of the form predicted by the droplet model. The exponents describing these fluctuations at and below T_c are indistinguishable within the accuracy of the calculation, which suggests that the transition is close to first order.

Acknowledgments

This work is supported by the US Israel Binational Foundation. APY would like to acknowledge support from the NSF through grant number DMR 9111576.

References

[1] Nattermann T and Villain J 1988 *Phase Trans.* **11** 817
[2] Belanger D P and Young A P 1991 *J. Magn. Magn. Mater.* **100** 272
[3] Bricmont J and Kupiainen A 1987 *Phys. Rev. Lett.* **59** 1829
[4] Villain J 1985 *J. Physique* **46** 1843
[5] Fisher D S 1986 *Phys. Rev. Lett.* **56** 416
[6] Bray A J and Moore M A 1985 *J. Phys. C: Solid State Phys.* **18** L927
[7] Schwartz M and Soffer A 1985 *Phys. Rev. Lett.* **55** 2499
[8] Casher A and Schwartz M 1979 *Phys. Rev.* B **18** 3440
[9] Migdal A A 1975 *Sov. Phys.–JETP* **42** 743
[10] Kadanoff L P 1976 *Ann. Phys.* **100** 359
[11] Schwartz M and Fishman S 1980 *Physica* A **104** 115
[12] Ogielski A T 1986 *Phys. Rev. Lett.* **57** 1251
[13] Belanger D P, King A R, Jaccarino V and Cardy J L 1983 *Phys. Rev.* B **28** 2522
[14] Southern B W and Young A P 1977 *J. Phys. C: Solid State Phys.* **10** 2179
[15] Kirkpatrick S 1977 *Phys. Rev.* B **16** 4630
[16] José J V, Kadanoff L P, Kirkpatrick S and Nelson D R 1977 *Phys. Rev.* B **16** 1217